River channel slope, flow resistance, and gravel entrainment thresholds

Robert I. Ferguson[1]

Received 28 April 2011; revised 20 March 2012; accepted 20 March 2012; published 10 May 2012.

[1] River beds are traditionally assumed to become mobile at a fixed value of nondimensional shear stress, but several flume and field studies have found that the critical value is higher in steep shallow flows. Explanations for this have been proposed in terms of the force balance on individual grains. The trend can also be understood in bulk-flow terms if total flow resistance has "base" and "additional" components, the latter due to protruding immobile grains as well as any bedforms, and the stress corresponding to "additional" resistance is not available for grain movement in threshold conditions. A quantitative model based on these assumptions predicts that critical Shields stress increases with slope, critical stream power is near-invariant with slope, and each has a secondary dependence on bed sorting. The proposed slope dependence is similar to what force-balance models predict and consistent with flume data and most field data. Possible explanations are considered for the inability of this and other models to match the very low critical values of width-averaged stress and power reported for some low-gradient gravel bed rivers.

Citation: Ferguson, R. I. (2012), River channel slope, flow resistance, and gravel entrainment thresholds, *Water Resour. Res.*, *48*, W05517, doi:10.1029/2011WR010850.

1. Introduction

[2] Bed load transport is highly intermittent in streams and rivers with beds consisting mainly of gravel, cobbles or boulders. Hardly any bed material moves until the flow exceeds a critical value of bed shear stress ($\tau = \rho g d S$, where ρ is water density, g the gravity acceleration, d the mean flow depth, and S the channel slope) or specific stream power ($\omega = \tau V$, where V is mean water velocity). Above this threshold the transport rate increases nonlinearly with excess stress or power. The combination of threshold and nonlinearity means that predictions of such things as duration of competent flow and total bed-material flux over a period are highly sensitive to the value used for critical stress or power, so guidelines for setting this are important to geomorphologists and other water scientists.

[3] The primary determinant is the typical size of the bed surface sediment. *Shields* [1936] showed experimentally that the threshold of motion of a plane bed occurs at a near-constant critical value (θ_c) of the nondimensional shear stress (or Shields stress) defined by

$$\theta = \frac{\tau}{(\rho_s - \rho)gD} = \frac{dS}{RD}, \quad (1)$$

where ρ_s denotes grain density, D is mean grain diameter (nowadays replaced by the median, D_{50}), and $R = (\rho_s - \rho)/\rho$ is the submerged specific gravity of the grains. Rivers are commonly assumed to have near-constant θ_c so long as D_{50} does not fall within the gap of a bimodal distribution and is greater than ~2 mm so that the grains protrude well above the laminar sublayer and the grain Reynolds number is high. A comprehensive review by *Buffington and Montgomery* [1997] showed that published estimates of θ_c for gravel bed rivers fell within a fairly narrow range (0.030 to 0.086) and that some of the variance could be attributed to differences in bed packing or in the operational definition of threshold of motion.

[4] In very steep channels the down-channel component of grain weight aids mobility, which by itself should reduce θ_c slightly, but there is strong evidence that θ_c as calculated using D_{50} and measured flow depth increases systematically with slope. This tendency was first noted by *Shields* [1936] and an increase from ~0.03 at low gradients to 0.05–0.08 at moderate gradients has been confirmed in many subsequent flume experiments [*Ashida and Bayazit*, 1973; *Bathurst et al.*, 1983, 1987; *Shvidchenko and Pender*, 2000; *Shvidchenko et al.*, 2001; *Parker et al.*, 2011]. Values of 0.10–0.16 at very high slopes can be inferred from experiments reported by *Armanini and Gregoretti* [2005]. High values of θ_c have also been reported from the field: *Mueller et al.* [2005] estimated values of up to 0.12 for steep gravel bed rivers, and *Mao et al.* [2008] estimated values of ~0.2 for two mountain torrents. Many of these authors suggested that the tendency for θ_c to be higher in steeper channels is linked to greater flow resistance as flow becomes shallower relative to bed material size, and some demonstrated a correlation between θ_c and the relative roughness D/d [e.g., *Bathurst et al.*, 1983; *Buffington and Montgomery*, 1997; *Shvidchenko and Pender*, 2000]. More recently, *Lamb et al.* [2008] and *Recking* [2009] presented

[1]Department of Geography, Durham University, Durham, UK.

0043-1397/12/2011WR010850

convincing mechanistic explanations of the trend by analyzing how changes in near-bed hydraulics in shallow flows affect the force balance on individual grains. Their microscale models necessarily contain several poorly constrained parameters, so that they predict families of curves rather than any unique relation between θ_c and slope, but with plausible parameter values the predictions agree quite well with flume and field data.

[5] This paper follows *Lamb et al.* [2008] and *Recking* [2009] in trying to explain the empirical association between critical stress, channel slope, and flow resistance in streams with coarse beds, but from a different perspective, as I focus on bulk flow properties rather than grain-scale mechanics. The approach is based on an analogy with the partitioning between grain and form components of resistance and shear stress in rivers with large bedforms such as dunes or bars. The intention is to support and complement the work of *Lamb et al.* [2008] and *Recking* [2009] by showing that similar results can be obtained from a macro rather than micro perspective. A further outcome is a new model for how, on average, critical stream power varies with slope. The predicted slope dependence of critical Shields stress and nondimensional critical power is in broad agreement with available flume and field data, with the exception of very low values that are reported for some field sites. Section 7 of the paper discusses this discrepancy as well as reviewing limitations and uncertainties of the approach and considering some of the implications of the increase in critical stress with channel slope.

2. Conceptual Model

[6] My starting point is the idea that some of the total shear stress in a river with a poorly sorted coarse bed is unavailable for grain entrainment because it is dissipated in overcoming resistance not associated with the grains that are potentially mobile in near-threshold conditions. This argument has been made by several previous authors [e.g., *Wiberg and Smith*, 1991; *Buffington and Montgomery*, 1997; *Mueller et al.*, 2005; *Yager et al.*, 2007] and is analogous to the widely accepted partitioning of total shear stress into components associated with "grain" and "form" roughness in rivers with macroscale bedforms. Some of the total shear stress is expended on the form drag induced by bedforms or obstacle clasts, leaving less available to move individual grains. The original way to allow for this was to predict bed load transport rate from only the effective part of the total shear stress after correcting for form drag [e.g., *Meyer-Peter and Müller*, 1948]. However, if the prediction equation contains a critical stress or reference stress, allowance for bedforms or obstacle clasts can equally well be made by using the total shear stress with a higher critical stress. The latter approach was taken in all of the post-1948 literature cited above and is followed here.

[7] Flow resistance in a channel of given slope and grain size distribution depends on how the grains are arranged, even in the absence of macroscale bedforms such as bars or dunes. For example, in the cartoons of Figure 1 the fine-scale standard deviation of bed elevation, which is known to be a good predictor of resistance [e.g., *Aberle and Smart*, 2003], increases from case A (grain tops aligned in a plane) to case B (grain centers aligned) and case C (grain bases aligned, maximum protrusion of larger grains above the general level). Flow resistance at any given depth will increase from A to B to C because of greater form drag on protruding clasts.

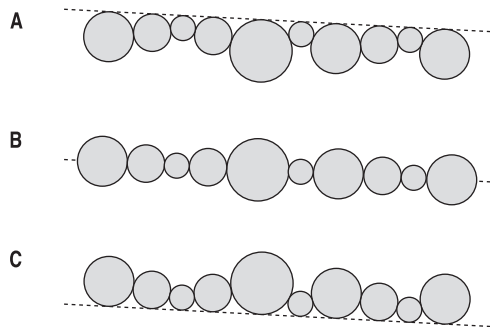

Figure 1. Alternative configurations of the same mixed-size river bed material with (a) minimum resistance to flow, and (b and c) higher resistance because of drag on protruding grains. Flow is left to right.

[8] Here the traditional low value of θ_c is assumed to apply only to beds with the relatively smooth water-worked microtopography that is typically generated in flume experiments at low Shields stress: not necessarily the idealized end-member of Figure 1a, but certainly between Figures 1a and 1b and without any macroscale bedforms or large immobile clasts. This near-minimal degree of bed irregularity, often called "grain roughness," generates what I call the "base" level of resistance, following the terminology of *Rickenmann and Recking* [2011]. The flow resistance in a stream or river with mixed grain sizes and shapes usually exceeds this base level, because even in the absence of large bedforms the microtopography tends to fall between Figures 1b and 1c. The end-member Figure 1c was assumed by *Wiberg and Smith* [1991] in their calculations of the effect of clast form drag on velocity profiles. The protruding grains which generate the additional resistance in Figures 1b and 1c are usually from the coarser half of the size distribution, and are unlikely to be mobile in near-threshold conditions since the evidence from field studies is that bed load is then predominantly fine-grained [e.g., *Wathen et al.*, 1995; *Ryan et al.*, 2005]. Part of the total shear stress is expended in overcoming the additional flow resistance created by these immobile coarse grains (and any bars, steps, dunes or other macroscale bedforms) so is not available for movement of other grains. The total stress at the onset of motion is therefore higher to an extent that depends on the ratio of total flow resistance to the base level of flow resistance. If this ratio varies with channel slope, so must θ_c.

[9] Several mechanistic models have been proposed for how near-bed flow and bed load transport is affected by a regular array of obstacles or a random arrangement of protruding grains [e.g., *Wiberg and Smith*, 1991; *Canovaro et al.*, 2007; *Yager et al.*, 2007; *Lamb et al.*, 2008; *Recking*, 2009]. This paper does not propose another model of this type; rather, it infers the effects of obstacles from the difference between the typical level of total flow resistance and the ideal base level of flow resistance associated with a bed that is almost as smooth as possible. A similar division into base resistance and additional resistance has been made by

Govers and Rauws [1986] and *Raupach et al.* [1993] in the context of soil erosion by overland flow and wind, respectively; *Millar* [1999] in an assessment of the proportion of nongrain resistance in gravel bed rivers; *Recking* [2009] in the above mentioned mechanistic model of the $\theta_c - S$ relation; and *Yager et al.* [2007] and *Rickenmann and Recking* [2011] in models for why transport rates in torrents are lower than is predicted using a traditional low value for θ_c. My aim in this paper, then, is to explore the implications of this bulk-flow approach and see to what extent they agree with empirical trends and mechanistic models.

3. A Quantitative Model

3.1. General Approach

[10] In a channel of specified slope S and grain-size distribution the total shear stress $\tau = \rho g d S$ can be divided into components associated with "base" and "additional" resistance by partitioning the observed mean flow depth d in the same way that *Einstein and Barbarossa* [1952] proposed for flow over bedforms. The mean velocity V of a stream depends on the balance between gravitational driving force and total flow resistance. If the driving force is represented by the shear velocity $u_* = (gdS)^{1/2} = (\tau/\rho)^{1/2}$, the total flow resistance can be expressed as

$$\frac{V}{u_*} = \frac{V}{(gdS)^{1/2}} = F\left(\frac{d}{k}\right), \tag{2}$$

where F is some monotonically increasing function and k is a roughness height that is usually scaled on a representative coarse-grain diameter such as D_{84} or D_{90}. Many different resistance equations can be expressed in this general form. Each is of course an idealized general tendency around which there will be considerable scatter; for example, the configurations in Figures 1a, 1b, and 1c would have different resistance and velocity at the same flow depth.

[11] Different velocities at the same depth imply different depths for the same velocity. In base-resistance conditions with little particle protrusion (approaching the case in Figure 1a) a given mean velocity V would occur at some lower mean depth d′, and thus a lower unit discharge $q = d'V$. Velocity and relative submergence would then be related by

$$\frac{V}{(gd'S)^{1/2}} = F'\left(\frac{d'}{k'}\right), \tag{3}$$

where the function F' may be different from F and k' may be smaller than k. The shear stress in this idealized case would be $\tau' = \rho g d' S$, and the Shields stress would be $\theta' = d'S/RD_{50}$. By hypothesis, only this part of the total stress is available for entrainment of the small grains that are potentially mobile in near-threshold conditions, and its critical value θ'_c at the threshold of significant motion is a constant with a low value as in the experiments of *Shields* [1936]. The apparent critical Shields stress as calculated from the actual flow depth d_c in threshold conditions is therefore

$$\theta_c = \theta'_c\left(\frac{d_c}{d'_c}\right). \tag{4}$$

[12] For plausible combinations of base and total flow-resistance functions the ratio d/d' (hence also θ/θ') increases as the relative submergence d/k decreases. Steep channels generally have coarse bed material and shallow flow, giving high d_c/d'_c and therefore also high θ_c.

[13] This generic model is developed below by using specific choices of base and total flow-resistance functions to derive a quantitative model for how, on average, θ_c should vary with S if the assumptions outlined above are valid. The results are then compared with the trends predicted by the mechanistic models of *Lamb et al.* [2008] and *Recking* [2009], and with estimates of critical stress at various slopes in flume experiments and river reaches.

3.2. Choice of Flow Resistance Equations

[14] Quantitative results can be obtained by specifying any suitable combination of flow-resistance functions F and F' and associated roughness heights k and k'. The key criteria in choosing the total-resistance function are a good fit to data, especially at the intermediate to low submergence ratios that are typical of threshold conditions in coarse-bedded streams, together with consistency with what is understood about the details of shallow flows. A good choice on both grounds is the variable-power flow resistance equation (VPE) of *Ferguson* [2007]. This uses $k = D_{84}$ and can be written as

$$\frac{V}{u_*} = \frac{a_1(d/D_{84})}{[(d/D_{84})^{5/3} + (a_1/a_2)^2]^{1/2}}, \tag{5}$$

where a_1 and a_2 are coefficients. *Ferguson* [2007] found that the best fit to a large set of flow measurements in very diverse conditions was obtained by setting a_1 to ~6.5 and a_2 to ~2.5. These round-number values are used here without any calibration to the flume runs and field sites used as test data later in the paper.

[15] The VPE is a bridging function between two asymptotes: $V/u_* = a_1(d/D_{84})^{1/6}$ for deep flows and $V/u_* = a_2\, d/D_{84}$ in shallow flows. The deep-flow asymptote is equivalent to the Manning-Strickler equation $V = d^{2/3}S^{1/2}/n$ with $n \propto D_{84}^{1/6}$. With $a_1 = 6.5$ it is almost indistinguishable at $d/D_{84} > 10$ from the logarithmic equation with $k = 3.5D_{84}$ that was proposed by *Hey* [1979]. The shallow-flow asymptote is a linear increase in V/u_* with d/D_{84}, which is consistent with the linear velocity profile expected within a roughness layer [*Nikora et al.*, 2001; *Gimenez-Curto and Corniero*, 1996, 2006]. An equivalent nondimensional hydraulic geometry relation was found by *Rickenmann* [1991], *Aberle and Smart* [2003], and *Zimmermann* [2010] to give a good fit to shallow-flow measurements. The VPE consequently allows for the differences in eddy viscosity and velocity profile between deep and shallow flows, and thereby gives more or less unbiased predictions of velocity throughout the natural range of channel slope and relative submergence (Figure 2). *Ferguson* [2007] found that the VPE marginally out-performed several other equations, including that of *Hey* [1979], in predicting within-bank stream velocity measurements at submergences of 0.1 to 80 and slopes from <0.001 to >0.2. The VPE also performed best in later comparative tests by *Ferguson* [2012] using a greatly extended data set and by *Rickenmann and Recking* [2011] using an even larger and almost wholly independent data

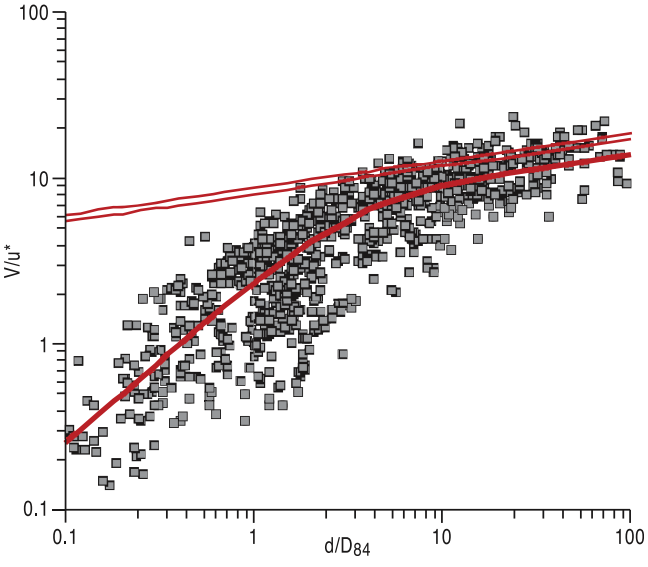

Figure 2. Relation between V/u_* (an inverse measure of total flow resistance) and relative submergence d/D_{84} in a set of 967 measurements of within-bank flows in gravel and boulder bed streams and rivers (data from numerous sources as listed in the work of *Ferguson* [2012], with sand bed reaches omitted). The bold curve is the VPE (equation (5) with $a_1 = 6.5$ and $a_2 = 2.5$) which is used to model total resistance. Its coefficients were calibrated to approximately one third of the data shown. The thin straight lines are the 1/6-power relation (equation (6) with $a_0 = 8.0$) used to model the base level of flow resistance, and shown here for $D_{84}/D_{50} = 1$ and 4.

set. For the data plotted in Figure 2 the VPE predicts velocity with mean and root-mean-square errors of -0.03 m s^{-1} and 0.52 m s^{-1}, respectively, compared to mean and rms errors of 0.55 m s^{-1} and 0.80 m s^{-1} for the logarithmic equation of *Hey* [1979].

[16] The base level of flow resistance is assumed to follow

$$\frac{V}{u_*} = a_0\left(\frac{d}{D_{50}}\right)^{1/6}, \tag{6}$$

with $a_0 = 8.0$. This is a power law approximation of the logarithmic relation

$$\frac{V}{u_*} = \frac{1}{\kappa}\ln\left(12.2\frac{d}{D_{50}}\right), \tag{7}$$

(where $\kappa \approx 0.41$ is von Karman's constant) which is widely used to describe the grain resistance of a plane bed on the assumption that the velocity profile is logarithmic. Equations (6) and (7) differ by less than $\pm 3\%$ for submergences from 6 to 100 and the power law form is mathematically convenient in the present analysis. As can be seen in Figure 2, (6) does provide an upper bound to observed values of V/u_* (i.e., a lower bound to flow resistance) with the exception of a few field estimates at intermediate to high values of relative submergence; it may, however, underestimate base resistance in extremely shallow flows. Sensitivity to the choices of total and base flow resistance functions is reviewed in the closing discussion.

3.3. Variation of Critical Shields Stress With Channel Slope

[17] As noted above a given velocity can be achieved with lower depth and unit discharge when there is less resistance to flow. The ratio d/d' of actual depth to theoretical base-resistance depth in a gravel bed river with an average level of total flow resistance can be obtained by equating V from the total resistance function (5) using depth d with V from the base resistance function (6) using depth d'. After some manipulation d/d' can be expressed as an explicit function of the relative roughness D_{84}/d:

$$\frac{d}{d'} = \left(\frac{a_0}{a_1}\right)^{3/2}\left(\frac{D_{84}}{D_{50}}\right)^{1/4}\left[1 + \left(\frac{a_1}{a_2}\right)^2\left(\frac{D_{84}}{d}\right)^{5/3}\right]^{3/4}. \tag{8}$$

[18] This predicts that as submergence increases in any particular reach d/d' declines toward an asymptotic value of $\sim$1.4 to $\sim$2 (depending on bed sorting) for deep flows. More importantly for present purposes it can also be applied between reaches at threshold flow stage. By setting up an array of values of the relative submergence d_c/D_{84} at threshold, (8) can be used to calculate corresponding values of d_c/d'_c. By the basic hypothesis of this paper, as embodied in equation (4), these are also values of θ_c/θ'_c. The corresponding array of slopes can now be calculated using

$$S = \frac{\theta_c R D_{50}}{d_c} = \frac{(\theta_c/\theta'_c)\theta'_c R}{(d_c/D_{84})(D_{84}/D_{50})} \tag{9}$$

with some low constant value of the base critical stress θ'_c. It is then possible to plot θ_c against S. The presence of D_{84}/D_{50} in (8) and (9) implies that the curve will shift according to bed sorting. In subsequent calculations the submerged specific gravity is taken as $R = 1.65$. The base value θ'_c of critical Shields stress is assumed to be 0.026, which is the average of the traditional value of 0.029 for uniformly packed spheres (G. Parker, 1D sediment transport morphodynamics with applications to rivers and turbidity currents, 2004, http://vtchl.uiuc.edu/people/parkerg/morphodynamics_e-book.htm chapter 6), the minimum value of 0.025 in flume data compilations plotted by *Shvidchenko and Pender* [2000], and the low-slope limit of 0.024 in the model of *Recking* [2009].

[19] The predicted pattern of how, on average, critical Shields stress increases with channel slope is illustrated in Figure 3a. "On average" here refers to what would be expected for reaches with total flow resistance exactly as predicted by the VPE (equation (5)); individual reaches with higher-than-average or lower-than-average bed roughness are expected to deviate from the VPE and therefore also from equation (8) and the curves in Figure 3. The central curve is for $D_{84}/D_{50} = 2$ which is a typical value for gravel bed rivers: 86% of 393 reaches listed by *Church and Rood* [1983] have $1.5 < D_{84}/D_{50} < 2.5$. The outer curves are for $D_{84}/D_{50} = 4$ which is exceptionally high (exceeded at only two of Church and Rood's sites) and $D_{84}/D_{50} = 1$ which is the asymptotic case of a perfectly uniform grain-size distribution and is approached in some flume experiments. It might be thought that the conceptual

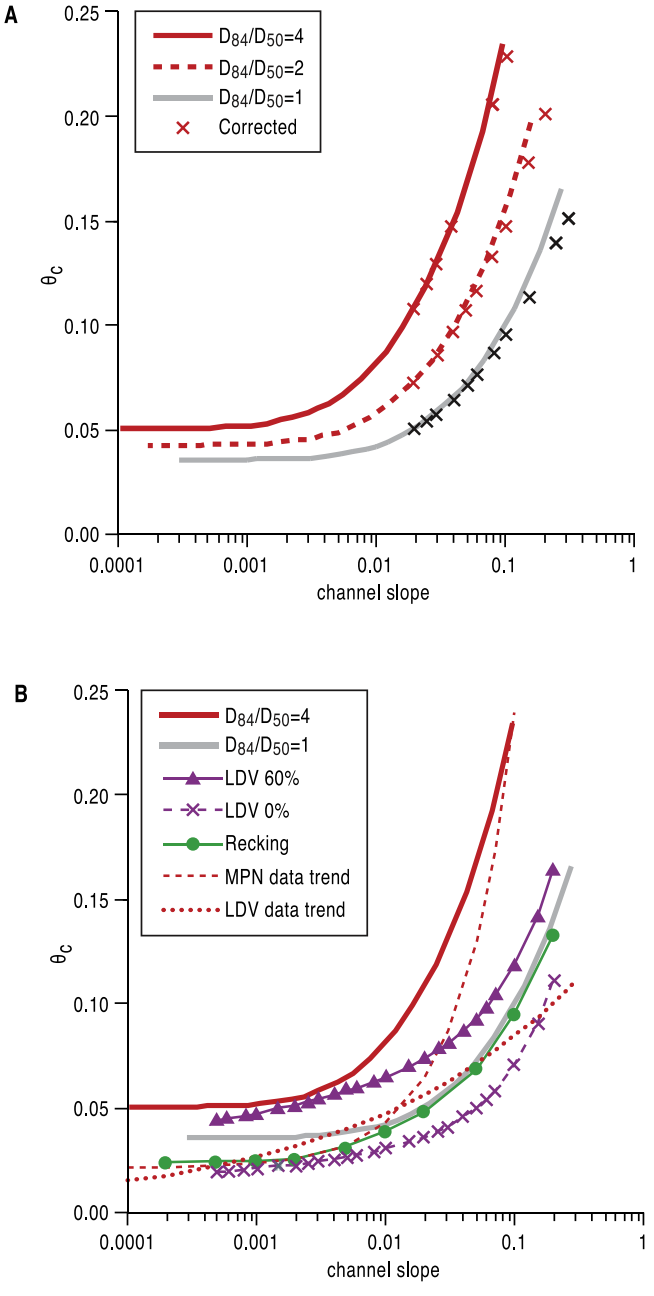

Figure 3. (a) Predicted increase in critical Shields stress θ_c with channel slope for natural river beds with typical levels of total flow resistance. Curves are shown for $D_{84}/D_{50} = 2$ and 4, and for the asymptotic case of a uniform grain-size distribution ($D_{84}/D_{50} = 1$). The crosses show the effect of correcting for the downslope component of grain weight. (b) Comparison of predictions for $D_{84}/D_{50} = 1$ and 4 with the models of *Lamb et al.* [2008] and *Recking* [2009]. The former is denoted by LDV and plotted for 0% and 60% contribution of what *Lamb et al.* [2008] termed "morphologic drag." The linear trend fitted to field data by *Mueller et al.* [2005], and the power law trend fitted to flume and field data by *Lamb et al.* [2008], are also shown.

model, which assumes an irregular bed surface, loses validity as D_{84}/D_{50} approaches 1; however, even a very narrow range of grain size as determined by sieving does not preclude substantial differences in grain shape and therefore in long-axis and short-axis lengths, permitting some irregularity in the elevations of grain tops.

[20] For each sorting ratio the critical stress is predicted to increase rather less than linearly with reach slope, but the curve rises more rapidly for less well-sorted beds. For any given degree of sorting, θ_c is predicted to increase by about a factor of four from lowland gravel bed rivers to mountain torrents. The effect of sorting is much smaller but still appreciable: at very low slopes θ_c is predicted to be ~20% higher for a typical natural bed ($D_{84}/D_{50} = 2$) than for a uniform bed, increasing to nearly 50% higher in very steep channels. This secondary dependence of critical stress on bed sorting will, however, be masked to some extent by the inherent scatter around the "typical" flow resistance as represented by the VPE. Approximate 90% bounds for the scatter in Figure 2 are given by VPE coefficients $a_1 = 4$ to 10 for deep flows and $a_2 = 1$ to 4 for shallow flows. Calculations using these values indicate that the resulting uncertainty in θ_c is asymmetric, with a lower bound only 10–20% below the central prediction for the appropriate value of D_{84}/D_{50} but an upper bound that is ~100% higher at very low slopes and ~70% higher at $S = 0.05$.

[21] Figure 3a also shows the effect of correcting the base value θ_c' of critical stress for the downslope component of grain weight, which aids grain mobility and thus reduces θ_c to some degree. The correction is

$$\theta_c' = \theta_{c0}'\left(1 - \frac{S}{\tan\alpha_f}\right)\cos\left(\tan^{-1}S\right), \tag{10}$$

(e.g., *Parker*, online, 2004, chapter 6) where $\theta_{c0}' = 0.026$ as above and α_f is the angle of friction for the median grain size, taken here as 52° for irregularly packed natural beds following *Johnston et al.* [1998]. The critical stress for a given slope now has to be obtained iteratively using trial values of d_c/D_{84}. Figure 3a shows that the correction makes no perceptible difference at slopes gentler than ~0.05 and reduces the critical stress by only a few per cent on the steepest slopes. Uncorrected calculations are used in the rest of the paper unless otherwise stated.

3.4. Comparison With Previous Work

[22] The curves predicted for uniform and very poorly sorted beds are repeated in Figure 3b in which they are compared with published empirical trend lines and with trends predicted by the mechanistic models of *Lamb et al.* [2008] and *Recking* [2009]. *Lamb et al.* [2008] treated what they called "morphologic drag," defined as "stress spent on collections of particles and other structures larger than grain scale," as a fixed user-specified proportion of total stress and did not allow for this proportion to vary with slope. They gave polynomial approximations for predictions with 0%, 40% and 60% morphologic drag. The 0% and 60% curves are plotted in Figure 3b as a likely envelope for natural conditions. Both curves are flatter than those predicted by the present model or by *Recking* [2009], and the 0% curve starts at a lower level ($\theta_c = 0.016$ at $S = 0.0001$). It may well be that the proportion of "morphologic drag"

tends to increase in the typically shallower flows in steeper reaches, giving a hybrid curve more like the predictions of *Recking* [2009] and the present model for well-sorted beds. However, the present model predicts higher critical stresses than either of the previous models in steep streams with poorly sorted beds.

[23] The empirical trend toward higher critical stress on steeper slopes has been fitted using either linear [*Mueller et al.*, 2005; *Recking*, 2009] or power law [*Pitlick et al.*, 2008; *Lamb et al.*, 2008; *Parker et al.*, 2011] regressions. Figure 3b shows that these diverge greatly when extrapolated to high slopes: the power law trend falls progressively below even the uniform-sediment predictions of the present model, whereas the linear trend of *Mueller et al.* [2005] gives a more rapid increase in critical stress with channel slope than the model predicts for any given bed sorting ratio. However, the field data used below to test the model show a significant positive correlation between D_{84}/D_{50} and channel slope, and taking this into account the model would predict a trend quite similar to what *Mueller et al.* [2005] fitted to their data. Model predictions for fixed bed sorting ratios can be matched fairly well by second-order polynomials but their best-fit coefficients are not related in any obvious way to the parameters θ_c' and D_{84}/D_{50}.

4. Comparison With Field and Flume Data

[24] The trends predicted by the model are now compared with those shown by estimates of critical stress for 43 field sites and in five sets of flume experiments. The data sources are listed in Table 1. They were selected with the aim of obtaining critical stresses for as wide a range of channel slopes as possible, but preferably using a common definition of "threshold of motion" since the estimated critical stress in a given river or flume experiment depends on how the threshold of significant motion is defined [*Buffington and Montgomery*, 1997] and the model predictions can best be tested if we minimize scatter due to methodological differences.

[25] The favored definition of threshold in most recent research is the flow that transports bed load at a predefined threshold or "reference" rate. Bed load is measured in a range of high flows with different shear stresses, a relation is fitted between transport rate and Shields stress, and the stress at which the reference transport rate is achieved is estimated by interpolation or extrapolation. Several experimentalists have used a reference rate of $\Phi = 0.0001$, where

$$\Phi = \frac{q_b}{\left(gRD_{50}^3\right)^{1/2}} \tag{11}$$

is Einstein's nondimensional transport rate, q_b is the volumetric transport rate per unit width and time, and D_{50} is based on bulk sieving. Field workers have generally used $W_* = 0.002$, where

$$W_* = \frac{\Phi}{\theta^{3/2}}, \tag{12}$$

which was first used by *Parker et al.* [1982]. The two definitions are equivalent only at a single high value of θ_c, so $W_* = 0.002$ usually corresponds to a slightly lower flow than $\Phi = 0.0001$. I adopted the latter definition here to make use of the laboratory results of *Shvidchenko and Pender* [2000], *Shvidchenko et al.* [2001], and *Parker et al.* [2011]. *Shvidchenko and Pender* [2000] found that Φ varied linearly with the proportion of grains moving per unit time, and that $\Phi = 0.0001$ corresponded to a transport intensity of about 1×10^{-4} s^{-1} as measured by image analysis. This implies only occasional movement of isolated grains, not continuous transport. In rivers with poorly sorted coarse beds threshold transport defined using either of these objective methods normally consists entirely of grains from the fine tail of the bed surface grain size distribution; often much or all of it is granules or sand. This supports the assumption that most of the bed surface is immobile, including all exposed grains of D_{50} and coarser size.

[26] The Idaho field data of *King et al.* [2004] were analyzed by *Mueller et al.* [2005] using $W_* = 0.002$ but I reanalyzed them using $\Phi = 0.0001$. For these sites, and all other field sites except those of *Mao et al.* [2008], I constructed a plot of log Φ against log θ from the raw data and fitted an equation to the major axis of the scatter using the bisector of y-on-x and x-on-y least-squares best-fit lines. I then calculated θ_c from the intersection of the major-axis equation with $\Phi = 0.0001$ after correcting for detransformation bias using the method of *Ferguson* [1986].

Table 1. Data Used to Test the Proposed Model for Critical Shear Stress and Critical Stream Power

Source	Number of Runs or Sites	Range of Slope	D_{84}/D_{50}	Threshold Definition
		Flume Experiments		
Shvidchenko and Pender [2000]	32	0.002–0.029	1.1	$\Phi = 0.0001$
Shvidchenko et al. [2001]	12	0.004–0.014	1.3–1.9	$\Phi = 0.0001$
Parker et al. [2011]	14	0.007–0.017	1.7	$\Phi = 0.0001$
Bathurst et al. [1987]	12	0.005–0.09	1.2	$\Phi = 0$
Armanini and Gregoretti [2005]	9	0.21–0.36	<1.1	visual onset
		Field Measurements		
King et al. [2004]	31	0.0005–0.051	1.4–4.2	$\Phi = 0.0001$
Bunte et al. [2008]	7	0.012–0.093	2.1–2.9	$\Phi = 0.0001$
Hollingshead [1971][b]	1	0.074	~3	$\Phi = 0.0001$
Jones and Seitz [1980][b]	2	0.00082, 0.00053	2.1, 1.9	$\Phi = 0.0001$
Mao et al. [2008]	2	0.136, 0.076	3.0, 4.0	tracer and trap D_{max}

[a]See text for details of how the threshold of transport was defined.
[b]Raw data obtained from *Gomez and Church* [1988].

Maximum measured transport rates were well below $\Phi = 0.0001$ at many sites, and four were excluded because the trend was insufficiently well defined to extrapolate with any confidence. At two sites with exceptionally steep $\Phi - \theta$ trends the regression method broke down and a visual trend line was used. My estimates of θ_c for the Idaho sites are highly correlated ($r = 0.91$) with those of *Mueller et al.* [2005] but are systematically higher because of the different definition of threshold.

[27] The D_{50} and D_{84} values for all field sites are based on pebble counts which included material <2 mm, and the measurements of *King et al.* [2004] and *Jones and Seitz* [1980] include all bed load coarser than 0.25 mm, but those of *Hollingshead* [1971] and *Bunte et al.* [2008] exclude bed load finer than 6 mm and 4 mm, respectively. This must tend to inflate the estimates of θ_c for these sites but the degree of bias will depend on bed load size distribution and could be accentuated or reduced by differences in trap efficiency.

[28] A few estimates of θ_c using different operational definitions of the threshold of motion are included in the test data set in order to extend the range of channel slopes. *Bathurst et al.* [1987] estimated critical depths in flume experiments by extrapolating transport-rate curves to zero, and *Armanini and Gregoretti* [2005] reported critical depths for the onset of motion as identified visually from video recordings of the bed of their flume. The critical stresses that I derived from these authors' results will be almost the same as for $\Phi = 0.0001$ since the latter corresponds to less than one grain moving per meter width per second in these experiments. Finally, the data set is completed by two values of θ_c taken from *Mao et al.* [2008]. These refer to steep torrents and were obtained using the competence-based method of *Andrews* [1983] in which the maximum grain size (D_{max}) that moves at various flow levels is regressed on τ or θ so that the stress required to move the bed D_{50} can be interpolated. *Buffington and Montgomery* [1997] found that competence-based estimates of θ_c are typically 15–30% lower than estimates based on $W_* = 0.002$, in which case the estimates for these torrents do correspond to Φ close to 0.0001.

[29] Figure 4 plots the data together with the trend curves predicted by the model. Flume and field data are plotted separately for clarity and the overall range of D_{84}/D_{50} (1.1–1.9 in the flume data, 1.4–4.2 in the field data) is stratified because of the predicted secondary influence of this parameter. The flume plot shows fairly good agreement between model and data. Runs with near-uniform sediment are scattered fairly symmetrically on either side of the "uniform" model curve, and runs with D_{84}/D_{50} closer to 2 all plot above the "uniform" curve but mostly below the upper curve. The field plot shows agreement in some respects but also some discrepancies. The model matches the trend of the *Bunte et al.* [2008] and "other" sites quite well, with all data points plotting either between the upper and lower

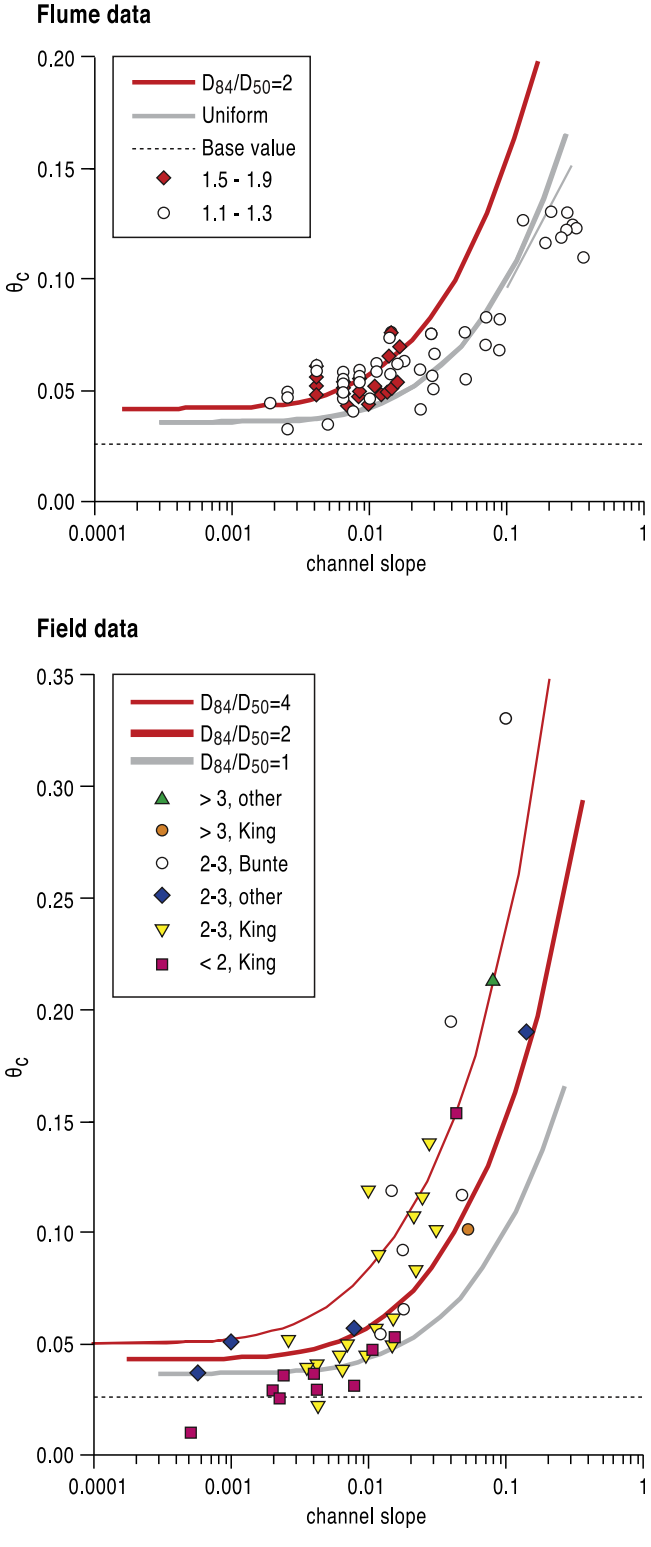

Figure 4. Comparison of flume and field estimates of critical Shields stress θ_c with the trends predicted for typical levels of total flow resistance and different values of channel slope and the bed sorting ratio D_{84}/D_{50}. The effect of correcting for the downslope component of grain weight is shown for the "uniform" ($D_{84}/D_{50} = 1$) curve in the flume plot (thin line branching off below the main curve). Data points are differentiated according to D_{84}/D_{50} as shown in the legends. Field data labeled "King" are Idaho sites in the work of *King et al.* [2004]; those labeled "Bunte" are sites in the work of *Bunte et al.* [2008] where only sediment coarser than 4 mm was trapped.

model curves (as expected) or only slightly outside them, though the two steepest sites of *Bunte et al.* [2008] are underpredicted. Some of the Idaho sites of *King et al.* [2004] are predicted well but there are two systematic discrepancies: the steeper reaches tend to have higher θ_c than the model suggests, and almost all of the low-slope reaches have lower θ_c than predicted. The discrepancy at low slopes is big in relative terms: there is one extreme outlier with θ_c estimated as only 0.009 and three others (two of them coincident in the plot) with estimated critical stresses that are lower than the minimum of 0.026 that is assumed here for "base" resistance.

[30] The predicted secondary dependence of θ_c on D_{84}/D_{50} is not clearly apparent in either plot, but a log-log multiple regression of the combined flume and field data does identify it. The best-fit trend is of the form $\theta_c \propto S^{0.32}(D_{84}/D_{50})^{0.23}$ with S significant at $p < 0.001$ and D_{84}/D_{50} significant at $p = 0.01$.

5. Extension to Critical Stream Power

[31] Although bed load transport rates are usually predicted from shear stress, some researchers and practitioners prefer to use stream power per unit bed area ($\omega = \tau V = \rho g Q S/w$, where w is water surface width) as the driver since it can be calculated from discharge and slope without needing to know the flow depth. The approach was developed by R. A. Bagnold in a series of papers [e.g., *Bagnold*, 1980]. The volumetric transport rate q_b is assumed to vary as $(\omega - \omega_c)^{3/2}$ where ω_c is a critical stream power. *Bagnold* [1980] used a Shields-type calculation of τ_c and a logarithmic resistance law for V to express ω_c as a function of grain size and depth. *Ferguson* [2005] pointed out some limitations of Bagnold's derivation and proposed alternative expressions for ω_c in which the depth dependence becomes an inverse dependence on slope. However, when *Parker et al.* [2011] calculated values of ω_c corresponding to the threshold transport rate $\Phi = 0.0001$ in their own and other workers' flume experiments they found no systematic variation with slope. They speculated that the inverse slope dependence predicted by *Ferguson* [2005] was balanced by a positive slope dependence of θ_c, which Bagnold and Ferguson had assumed to be constant.

[32] The model for critical stress that was developed in section 3 is easily extended to predict critical power. Critical power is assumed to be the product of critical stress and velocity at critical depth:

$$\omega_c = \tau_c V_c = \frac{\tau_c^{3/2}}{\rho^{1/2}}\left(\frac{V_c}{u_{*c}}\right). \tag{13}$$

[33] After substituting from equations (5), (8), and (9) this becomes

$$\omega_c = a_1\left(\frac{a_0}{a_1}\right)^{9/4}\left(\frac{D_{84}}{D_{50}}\right)^{3/8}(\rho R g D_{50})^{3/2} \times (\theta_c')^{3/2}\frac{[1+(a_1/a_2)^2(D_{84}/d_c)^{5/3}]^{5/8}}{(D_{84}/d_c)^{1/6}}. \tag{14}$$

[34] Critical stream power therefore increases with D_{50} and θ_c', as expected, but its precise value also depends on the relative roughness at the threshold of motion (D_{84}/d_c) and thus implicitly on slope. The nature of the implicit slope dependence is not obvious from (14) but can be revealed by finding the critical value of a nondimensional version of stream power for each of a range of slopes. A convenient scaling is

$$\omega_* = \frac{\omega}{\rho(gRD_{50})^{3/2}}, \tag{15a}$$

which was proposed by *Parker et al.* [2011] as a way of comparing empirical estimates of critical power in experimental studies with different values of D_{50}. Just as ω can be expressed as the product of shear stress τ and velocity V, so can ω_* be calculated from Shields stress and relative velocity:

$$\omega_* = \theta^{3/2}\frac{V}{u_*}. \tag{15b}$$

[35] Using (15b) a curve of critical nondimensional stream power ω_{*c} as a function of channel slope is obtained directly from the calculations used to construct Figure 3, since θ_c was obtained from d_c/D_{84} and V_c/u_{*c} also depends on this.

[36] Figure 5 shows how ω_{*c} is predicted to vary, on average, with slope and how the predicted values compare with empirical values for flume experiments and rivers. The test data are the same as in Figure 4 and Table 1 except that ω_{*c} cannot be calculated for the *Armanini and Gregoretti* [2005] experiments (for lack of information on q or V) and some field sites are excluded because plots of Φ against ω_* did not have a sufficiently well-defined trend to be extrapolated confidently to the $\Phi = 0.0001$ threshold.

[37] The model predicts that, as channel slope increases, ω_{*c} initially declines slightly to a minimum at a slope of $\sim$0.005 and then increases gradually. Correction for the downslope component of particle weight makes negligible difference until $S \sim 0.05$, above which the uncorrected curves continue to rise but the corrected curves flatten off and eventually fall. The curve shifts upward and slightly leftward for less well-sorted beds: the minimum value of ω_{*c} increases from 0.07 to 0.12 as D_{84}/D_{50} increases from 1 to 4, and the maximum of the corrected curve at high slopes increases from 0.11 to 0.28. The typical value of nondimensional critical power is therefore predicted to be constant to within a factor of $\sim$2 for a given bed sorting ratio, or within a factor of $\sim$4 over the full range of slopes and bed sorting. On average ω_{*c} is predicted to be of order 0.1, which is also what *Parker et al.* [2011] suggested as a rule of thumb in the absence of any obvious correlation of ω_{*c} with slope in their compilation of flume data.

[38] The estimated values of ω_{*c} show more scatter than the model predictions, as expected since the model is for typical levels of total flow resistance and individual river reaches and flume runs may have smoother or rougher beds than is typical at the slope concerned. The crucial tests are whether the data support the predicted small and nonmonotonic variation of θ_c with slope and whether the model correctly predicts the general level of critical power. As was found when considering critical shear stress (Figure 4), Figure 5 shows generally good agreement with the exception

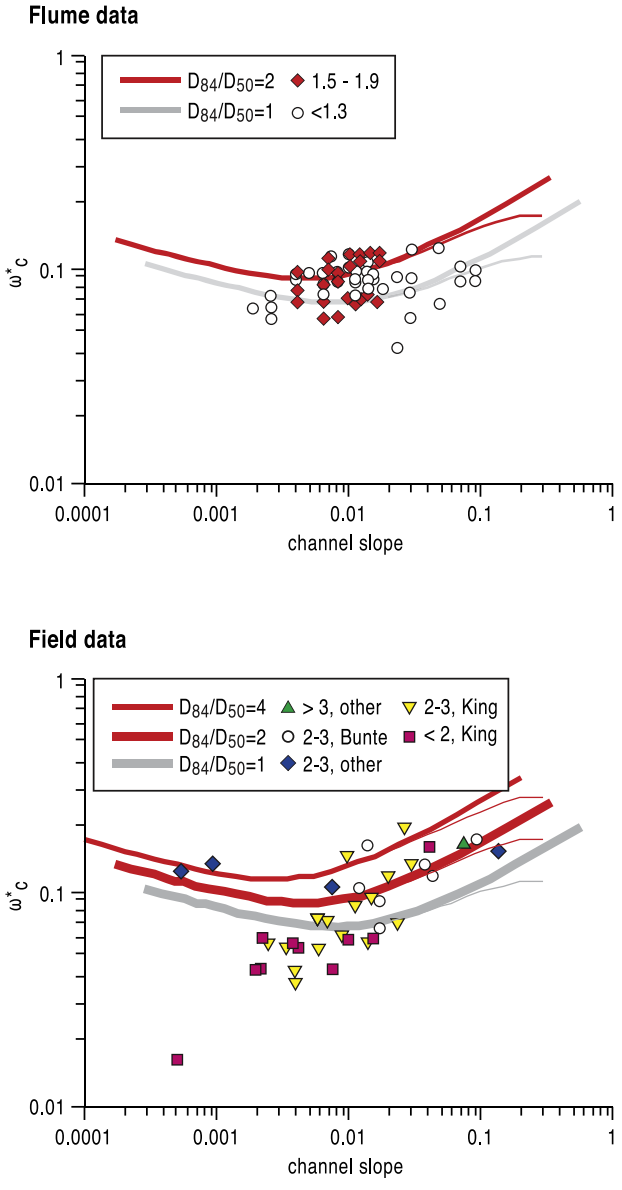

Figure 5. Comparison of flume and field estimates of critical nondimensional stream power ω_{*c} with those predicted for typical levels of total flow resistance and different values of channel slope and the bed sorting ratio D_{84}/D_{50}. The thinner lines branching off below the main curves at high slopes show the effect of correcting for the downslope component of particle weight. Data points are differentiated by D_{84}/D_{50} and source as in Figure 4.

of the *King et al.* [2004] field data. No flume data are available for very low or very high slopes, so the predicted tendency for ω_{*c} to be lowest at intermediate slopes cannot be tested, but the general level of ω_{*c} over the observed range of slopes is correctly predicted: approximately half of the flume data points fall between the model curves, the remaining points are fairly evenly scattered above and below the expected band, and the less well sorted beds plot slightly higher on average. The field data cover a wider range of slopes. The model predicts the general level of ω_{*c} for the *Bunte et al.* [2008] and "other" field data sets quite well, and likewise for the steeper reaches in the *King et al.* [2004] Idaho data set, but there is little sign of any systematic shift according to D_{84}/D_{50}. The biggest discrepancy once again is that the lower-gradient Idaho reaches plot well below what the model predicts. The Idaho data set as a whole has a much lower median value of ω_{*c} (0.06) than the other field data (0.13) or the flume data (0.09). The low values of critical power at these sites are a consequence of the low values of estimated critical stress that were apparent in Figure 4, rather than abnormally low velocities at threshold, and the outlier with ω_{*c} <0.02 is the same site as the outlier in Figure 4. These low values of critical stress are discussed below.

6. Discussion

6.1. Model Limitations and Uncertainties

[39] The model developed in this paper takes a stress-partitioning approach that has many precedents; the novelty is to use "total" and "base" flow resistance equations to estimate the proportion of total shear stress that is unavailable for bed load transport in threshold conditions. This is a much less mechanistic approach than was taken by *Lamb et al.* [2008] and *Recking* [2009], who analyzed the force balance on individual grains, though there is one similarity insofar as *Recking* [2009] used flow-resistance data to constrain one of the parameters in his model.

[40] The comparisons of model predictions with flume and field data (Figures 4 and 5) show that even though the approach is not physically rigorous, it cannot be rejected as making unrealistic predictions. It does not give the same physical insight as mechanistic models, nor can it be used to make quantitative predictions of just what the threshold of motion will be for a particular bed configuration, but when made operational using the chosen pair of base and total flow resistance equations it does reproduce the general trends of variation in θ_c and ω_{*c} with channel slope. This adds a new source of support to the many previous suggestions that the tendency for θ_c to increase with slope is connected to the generally greater flow resistance in shallower streams.

[41] Although the conceptual argument is not tied to any particular pair of equations for total and base flow resistance the quantitative predictions do depend on this choice. Any combination other than equations (5) (VPE) and (6) (1/6-power of d/D_{50}) requires iterative solution of d/d' for each of a range of values of relative submergence in order to compute the curve of θ_c against S. The obvious alternative for total resistance is *Hey*'s [1979] logarithmic function with $k = 3.5D_{84}$ for total resistance, and the obvious alternative for base resistance is equation (7) (log law with $k = D_{50}$) which gives a much closer bound to the shallow-flow data in Figure 2. Calculations using these alternatives individually and in combination show that they do not perform as well as equations (5) and (6). Logarithmic total resistance with 1/6-power base resistance gives almost the same critical stresses at low gradients but a slower increase thereafter, so that the predicted values at high gradients are about 15% lower. This gives an inferior fit to the field data. Logarithmic base resistance with VPE total resistance makes next to no difference at slopes up to ~0.01 but at higher gradients θ_c is predicted to increase more slowly and, for uniform beds, eventually decreases after reaching a

maximum of only ~0.07. This is completely inconsistent with both flume and field data. Logarithmic functions for both total and base resistance gives similar θ_c to the VPE and 1/6-power model at low slopes but the curves rise substantially more slowly, with θ_c almost 50% lower at high gradients. This again is inconsistent with the data.

[42] Using D_{84} rather than D_{50} in either of the base-resistance equations obviously makes no difference to predictions for uniform beds but causes a downward shift of curves for less well sorted beds. The shift in predicted critical stress is of order 0.01–0.02 so is relatively large at low gradients but not at high gradients.

[43] The VPE has been shown to perform well on average for coarse-bedded streams of any slope but it makes no special allowance for large woody debris, boulder steps, submerged vegetation, or exposed bedrock. It appears to predict resistance in step-pool reaches in a fairly unbiased way (many of the data points at the left-hand side of Figure 2 are from such sites) but reaches with significant amounts of woody debris or riparian vegetation probably have greater total flow resistance, and by implication higher θ_c, than is predicted by the VPE with its default coefficients. It is possible to analyze the effect of steps and large woody debris on stream hydraulics and bed load transport using stress partitioning [e.g., *Manga and Kirchner*, 2000; *Wilcox et al.*, 2006] but allowing for these sources of additional resistance is beyond the scope of this paper.

[44] Another limitation which has been emphasized throughout the paper is that the VPE predicts only the typical level of flow resistance for a given submergence. The vertical scatter around the VPE curve in Figure 2 shows that velocity at individual sites can differ from the trend value by at least a factor of 2, and there is a correspondingly large horizontal scatter which is what is relevant to the estimation of d/d' (equation (8)) and hence the critical stress. As was noted in section 3.3 my uncertainty analysis suggests that θ_c could be somewhat lower, and substantially higher, than the trends plotted in Figures 3 and 4. If a reach was known to have an unusually rough or smooth bed, the implications for θ_c could be modeled by adjusting the VPE coefficient a_1 (in cases of high relative submergence) or a_2 (for high relative roughness) that is used in equation (8).

[45] Although the predictions of the model are subject to these qualifications and uncertainties, existing approaches to predicting critical stress are equally uncertain. The mechanistic models of *Lamb et al.* [2008] and *Recking* [2009] contain parameters which cannot be tightly constrained, and as noted in section 3.4 the empirical linear and power law regressions fitted by several authors diverge greatly when extrapolated to higher gradients than were present in the data sets.

6.2. What Are the Effects of Bed Sorting on Critical Stress and Critical Power?

[46] As was illustrated by the multiple curves in Figures 3a and 4, the model developed in this paper predicts that θ_c in a stream with typical flow resistance not only increases with channel slope but also has a secondary dependence on bed sorting as quantified by D_{84}/D_{50}. This dependence arises mathematically because the length scale for θ_c is D_{50} whereas the length scale for total flow resistance is D_{84}. It is implicit in the work of *Recking*'s [2009] mechanistic model of the $\theta_c - S$ relation for poorly sorted beds, and also in the theoretical work of *Wiberg and Smith* [1991] who showed that the near-bed velocity in the configuration of the present Figure 1c is sensitive to D_{84} when D_{50} is fixed, but insensitive to D_{50} when D_{84} is fixed.

[47] If critical stress depends on bed sorting, critical stream power also depends on sorting. The prediction is that θ_c and ω_{*c} will on average be higher for less well sorted beds, though as noted in section 3.3 the expected range of scatter around the "average" prediction for a given sorting ratio is of comparable magnitude to the difference between predicted "average" θ_c for uniform and very poorly sorted beds. The comparisons with flume and field data in Figures 4 and 5 do not show strong evidence of the predicted effect but regression analysis of the data does suggest a statistically significant effect. This equivocal result could just be because the effect is masked by scatter to a considerable extent, but the possibility should also be considered of some systematic factor acting in the opposite direction. One such factor which is important for the force balance on individual grains is the extent to which they have to climb out of pockets for entrainment to occur. Distributions of pocket angles in natural beds are very wide whatever the sorting, but there is a general tendency for poorer sorting to be associated with smaller pocket angles because fine grains can infill the deeper pockets [*Buffington et al.*, 1992; *Johnston et al.*, 1998]. With all else equal, smaller pocket angles imply lower critical stress so this could provide a microscale counter to the macroscale effect of greater flow resistance. The balance between the effects is likely to depend on bed packing arrangement.

6.3. Why Do Some Rivers Have Very Low Thresholds of Motion?

[48] One of the fundamental assumptions of the model is that θ_c has a nonzero minimum value for an ideally smooth bed: 0.026 in the calculations that generated Figures 3–6. Mechanistic models also imply minimum values of θ_c: 0.024 at $S < 0.001$ according to *Recking* [2009], or 0.016 at $S = 0.0001$ and 0.021 at $S = 0.001$ according to *Lamb et al.* [2008] in the case of no morphologic drag. Yet according to *Mueller et al.* [2005] seven of the 32 Idaho sites in the data set of *King et al.* [2004] have lower critical stresses than predicted by any of these models, and four of them still do in the present reanalysis with threshold defined by $\Phi = 0.0001$ rather than $W_* = 0.002$. One site has a particularly low value: $\theta_c = 0.008$ according to *Mueller et al.* [2005], or 0.009 in my reanalysis. The inability of any model to match these very low observed values calls for discussion.

[49] A discrepancy between theory and observation only discredits the theory if the observation is reliable and was made in a situation that does not conflict with any auxiliary assumption of the theory. Inspection of the raw data for the Idaho rivers reveals the usual wide scatter in the $\Phi - W_*$ and $\Phi - \theta$ plots, giving substantial uncertainty in estimates of θ_c, but the four sites in question would have very low values of θ_c on any interpretation of the plots. There are, however, two respects in which the field situation may not be directly comparable with the model. The model uses width-averaged values of all relevant variables, which should be satisfactory for comparisons with flume experiments, but

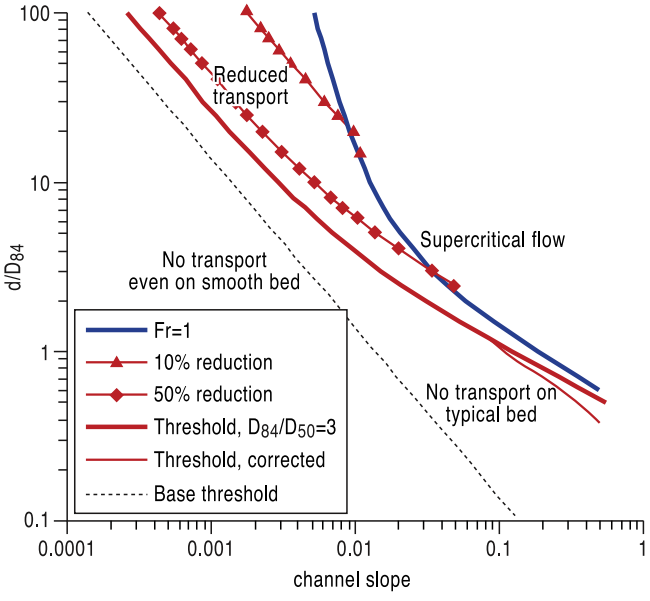

Figure 6. The predicted extent to which additional resistance in shallow flows affects the occurrence and rate of bed load transport at different combinations of channel slope and relative submergence (d/D_{84}). The straight broken line is the assumed threshold of motion (θ'_c) in conditions of base flow resistance, the next curve up is the predicted threshold (θ_c) in rivers with typical levels of total flow resistance, and the uppermost curve marks the onset of supercritical flow (Fr = 1). The curves with symbols are contours of 10% and 50% reduction in transport rate due to additional resistance.

many natural stream channels have nonrectangular cross sections and some have patches of locally coarser or finer sediment. Channel shape is relevant because θ_c calculated using mean depth and width-averaged transport rate may be misleadingly low if transport is in fact concentrated in the talweg or some other part of the cross section with locally high shear stress. This may be the case at the sites in question, since the maximum depth at the estimated threshold of motion exceeds the mean depth by 50% at the site with lowest estimated θ_c and by 25–70% at the other three. Patchiness is relevant because θ_c is calculated using reach-averaged bed surface D_{50}, which ranges from 67 to190 mm in the four reaches in question, but the bed load at each site is dominated by coarse sand (0.5–2 mm) according to *King et al.* [2004, Table 10] and inspection of the raw data. This suggests the load is either overpassing from upstream or is entrained mainly from fine patches within the reach, as has been observed elsewhere [e.g., *Garcia et al.*, 1999]. It may be relevant that the sites with very low critical stress and power are all quite large rivers, which possibly gives more opportunity for spatial variation in bed texture. If the load is derived from upstream the threshold has not yet been attained within the reach, and if the load is derived from fine patches scaling shear stress by the overall D_{50} gives a lower value of θ_c than would be correct for the mobile patches. Either way the stress required to mobilize the bed D_{50} would inevitably be higher than is estimated from the overall transport rate. To determine it accurately requires analyzing transport rates of individual size fractions, as first done by *Parker et al.* [1982].

[50] It is impossible to tell from the available data whether these differences between spatially averaged models and spatially variable reality can fully account for the shortfall between observed and predicted critical stresses, but they probably go some way to explaining the discrepancy. A reduction in typical pocket angles as a result of infilling by the high volumes of sand transported by these rivers is another possibility: although the published bed surface grain-size distributions for the sites do not indicate any significant amount of sand on the surface, the low-gradient sites within the Idaho batholith typically have sand exposed in marginal bars and recirculation zones, and some have narrow sand ribbons (J. Buffington, personal communication, March 2012).

6.4. Implications of the Increase in Critical Stress With Channel Slope

[51] Floods in steep streams can convey enough bed load to have major practical consequences, but the volumes involved are often much smaller than is predicted by conventional transport laws that seem to work for larger rivers on lower gradients [*Bathurst et al.*, 1987; *d'Agostino and Lenzi*, 1999; *Rickenmann*, 2001; *Chiari and Rickenmann*, 2011]. Some authors have speculated that this is the result of dissipating some of the total stress on additional resistance [e.g., *Rickenmann*, 2001; *Yager et al.*, 2007] and others have emphasized the importance of an increase in θ_c through bed structuring as a stabilizing factor [e.g., *Church et al.*, 1998].

[52] The model developed above offers a new perspective on the extent to which bed load transport is inhibited in steep streams. Figure 6 shows the space of possible combinations of channel slope and relative submergence d/D_{84}. Shear stress, stream power, and their nondimensional equivalents all increase upward in this diagram when considering a particular reach with given slope and bed composition, or diagonally upward and rightward when different reaches are compared. The Froude number of the flow also increases upward and rightward and the curve of Fr = 1 is shown as an upper limit to likely combinations of slope and relative roughness in alluvial channels [*Grant*, 1997].

[53] The space below the Fr = 1 curve is divided into regions using the predicted threshold of motion for an unusually smooth bed (base resistance, traditional low constant value of θ_c) and the predicted threshold for typical total flow resistance. The vertical separation between the two threshold curves corresponds to the range of flow depths at which transport is almost completely suppressed by typical amounts of additional flow resistance. It increases with channel slope. Even at low slopes ($S \sim 0.001$) the predicted flow depth required to transport bed load in a river with typical flow resistance is about twice the depth required in a river with only the base level of resistance, and at slopes of ~0.05 the ratio is almost 5. In even steeper channels bed movement is restricted to a narrow range of hydraulically subcritical flows, as can be seen by how close the threshold curve is to the Fr = 1 curve. The curve shown is for a poorly sorted bed ($D_{84}/D_{50} = 3$); with D_{84}/D_{50} much below 2, the threshold curve actually crosses into the supercritical flow zone.

[54] Finally, the area between the model threshold and Fr = 1 is divided by contours of 10% and 50% reduction in bed load flux when allowance is made for additional flow resistance. These contours were computed by assuming that transport rates follow an excess-stress law of the form

$$\Phi \propto (\theta - \theta_c)^{3/2} \tag{16}$$

[e.g., *Meyer-Peter and Müller*, 1948]. The ratio of bed load flux allowing for additional resistance to the flux with only base resistance is then given by

$$\frac{\Phi}{\Phi'} = \frac{(\theta - \theta_c)^{3/2}}{(\theta - \theta_c')^{3/2}} \tag{17}$$

for $\theta > \theta_c$. This can be rearranged and combined with equations (8) and (9) to compute the slope giving a specified % reduction in flux at any given submergence. The symbols defining the contours in Figure 6 represent slope values calculated in this way for an array of submergence values. It can be seen that transport rates in channels steeper than $S = 0.01$ are at least 10% lower than would traditionally be predicted, and at least 50% lower in very steep channels.

7. Conclusions

[55] The observed increase in critical Shields stress with channel slope, which *Lamb et al.* [2008] and *Recking* [2009] have explained mechanistically in terms of near-bed hydraulics and grain force balance, can also be understood as a consequence of how bulk flow resistance tends to increase in shallower flows on steeper slopes. The approach relies on a stress-partitioning argument analogous to that which has long been used for flows over bedforms. Predictions of critical Shields stress and critical nondimensional stream power derived from this approach agree fairly well with the trends of flume test data and most field data if total flow resistance is represented by the variable-power equation of *Ferguson* [2007].

[56] The model also predicts a secondary dependence of critical stress on the D_{84}/D_{50} ratio. The evidence for this is equivocal, partly because the uncertainty of predicted θ_c due to scatter around the flow resistance curve is of similar magnitude to the predicted effect of bed sorting and possibly also because of the opposite effect of differences in pocket-angle distributions.

[57] The predicted increase in θ_c with slope for given bed sorting is neither linear nor a simple power law, but if D_{84}/D_{50} increases with slope, as is the case in the test data, the overall effect is close to a linear increase in θ_c with slope and not dissimilar to the predictions of mechanistic models.

[58] A new model for critical stream power is obtained as a by-product. It predicts that critical power does not vary monotonically with slope and nondimensional critical power has a narrow range of typical values. The test data support these predictions.

[59] The very low values of critical stress and critical power that have been estimated for some field sites cannot be explained by this or other models. They may to some extent be biased downward by the effects of lateral variation in shear stress and transport rate, and by overpassing of bed load entrained from small patches of material finer than the bed as a whole.

[60] **Acknowledgments.** Kristin Bunte is thanked for providing raw data from streams in CO and WY, Erich Mueller for providing his estimates of critical power in ID rivers, and Chris Parker for making available values of critical stress and power for his own and other flume experiments. All three were generous with information and clarification. Wide-ranging critiques of earlier versions of the paper by Erich Mueller, John Buffington, and two anonymous reviewers helped the author sharpen the central argument and data analysis and improve the way in which they are explained. Chris Orton produced the diagrams.

References

Aberle, J., and G. M. Smart (2003), The influence of roughness structure on flow resistance on steep slopes, *J. Hydraul. Res.*, *41*(3), 259–269.

Andrews, E. D. (1983), Entrainment of gravel from naturally sorted riverbed material, *Geol. Soc. Am. Bull.*, *94*, 1225–1231.

Armanini, A., and C. Gregoretti (2005), Incipient sediment motion at high slopes in uniform flow condition, *Water Resour. Res.*, *41*, W12431, doi:10.1029/2005WR004001.

Ashida, K., and M. Bayazit (1973), Initiation of motion and roughness of flows in steep channels, in *Proceedings of 15th Congress International Association Hydraulic Research*, vol. 1, pp. 475–484, Int. Assoc. for Hydraulic Res., Istanbul, Turkey.

Bagnold, R. A. (1980), An empirical correlation of bedload transport rates in flumes and natural rivers, *Proc. R. Soc. London A*, *372*, 453–473.

Bathurst, J. C., W. H. Graf, and H. H. Cao (1983), Initiation of sediment transport in steep channels with coarse bed material, in *Mechanics of Sediment Transport*, edited by B. M. Sumer, and A. Muller, pp. 207–213, Balkema, Chichester, UK.

Bathurst, J. C., W. H. Graf, and H. H. Cao (1987), Bed load discharge equations for steep mountain rivers, in *Sediment Transport in Gravel Bed Rivers*, edited by C. R. Thorne, J. C. Bathurst, and R. D. Hey, pp. 453–491, Wiley, Chichester, UK.

Buffington, J. M., and D. R. Montgomery (1997), A systematic analysis of eight decades of incipient motion studies with special reference to gravel bedded rivers, *Water Resour. Res.*, *33*(8), 1993–2029.

Buffington, J. M., W. E. Dietrich, and J. M. Kirchner (1992), Friction angle measurements on a naturally formed gravel streambed: Implications for critical shear stress, *Water Resour. Res.*, *28*, 411–425.

Bunte, K., S. R. Abt, J. P. Potyondy, and K. W. Swingle (2008), A comparison of coarse bedload transport measured with bedload traps and Helley-Smith samplers, *Geodin. Acta*, *21*, 53–66.

Canovaro, F., E. Paris, and L. Solari (2007), Effects of macro-scale bed roughness geometry on flow resistance, *Water Resour. Res.*, *43*, W10414, doi:10.1029/2006WR005727.

Chiari, M., and D. Rickenmann (2011), Back-calculation of bedload transport in steep channels with a numerical model, *Earth Surface Proc. Landf.*, *36*, 805–815.

Church, M., and K. Rood (1983), *Catalogue of Alluvial Channel Regime Data*, 99 pp., Dep. of Geogr., Univ. of B. C., Vancouver, Canada. [Available at http://www.nced.umn.edu/].

Church, M., M. A. Hassan, and J. F. Wolcott (1998), Stabilizing self-organized structures in gravel bed stream channels: field and experimental observations, *Water Resour. Res.*, *34*, 3169–3179.

D'Agostino, V., and M. A. Lenzi (1999), Bedload transport in the instrumented catchment of the Rio Cordon, part II: Analysis of the bedload rate, *Catena*, *36*, 191–204.

Einstein, H. A., and N. L. Barbarossa (1952), River channel roughness, *Trans. Am. Soc. Civ. Eng.*, *117*, 1121–1146.

Ferguson, R. I. (1986), River loads underestimated by rating curves, *Water Resour. Res.*, *22*, 74–76.

Ferguson, R. I. (2005), Estimating critical stream power for bedload transport calculations in gravel bed rivers, *Geomorphology*, *70*, 33–41.

Ferguson, R. (2007), Flow resistance equations for gravel and boulder bed streams, *Water Resour. Res.*, *43*, W05427, doi:10.1029/2006WR005422.

Ferguson, R. (2012), Reach-scale flow resistance, in *Treatise on Geomorphology, Fluvial Geomorphology*, edited by J. Schroder and E. Wohl, (Elsevier, New York), Chap. 9.5, vol. 9, in press.

Garcia, C., J. Laronne, and M. Sala (1999), Variable source areas of bedload in a gravel bed stream, *J. Sediment. Res.*, *69*, 27–31.

Gimenez-Curto, L. A., and M. A. Corniero Lera (1996), Oscillating turbulent flow over very rough beds, *J. Geophys. Res.*, *101*(C9), 20,745–20,758.

Gimenez-Curto, L. A., and M. A. Corniero (2006), Comment on "Characteristic dimensions of the step-pool bed configuration: An experimental study" by Joanna C. Curran and Peter R. Wilcock, *Water Resour. Res.*, *42*, W03601, doi:10.1029/2005WR004296.

Gomez, B., and M. Church (1988), *A catalogue of equilibrium bedload transport data for coarse sand and gravel bed channels*, 90 pp., Dep. of Geogr., UBC, Vancouver, Canada.

Govers, G., and G. Rauws (1986), Transporting capacity of overland flow on plane and on irregular beds, *Earth Surface Processes Landforms*, *11*, 515–524.

Grant, G. E. (1997), Critical flow constrains flow hydraulics in mobile-bed streams: A new hypothesis, *Water Resour. Res.*, *33*, 349–358.

Hey, R. D. (1979), Flow resistance in gravel bed rivers, *J. Hydraul. Div. ASCE*, *105*, 365–379.

Hollingshead, A. B. (1971), Sediment transport measurements in a gravel river, *J. Hydraul. Div. ASCE*, *97*, 1817–1834.

Johnston, C. E., E. D. Andrews, and J. Pitlick (1998), In situ determination of particle friction angles of fluvial gravel, *Water Resour. Res.*, *34*, 2017–2030.

Jones, M. L., and H. R. Seitz (1980), Sediment transport in the Snake and Clearwater Rivers in the vicinity of Lewiston, Idaho, *U.S. Geol. Surv. Open-File Rep., 80-690*, 179 pp., U.S. Geol. Surv., Boise, Idaho.

King, J. G., W. W. Emmett, P. J. Whiting, R. P. Kenworthy, and J. J. Barry (2004), Sediment transport data and related information for selected coarse-bed streams and rivers in Idaho, *U.S. For. Serv. Tech. Rep. RMRS-GTR-131*, 26 pp., U.S. Dept. of Agric., Fort Collins, Colo.

Lamb, M. P., W. E. Dietrich, and J. G. Venditti (2008), Is the critical Shields stress for incipient sediment motion dependent on channel-bed slope?, *J. Geophys. Res.*, *113*, F02008, doi:10.1029/2007JF000831.

Manga, M., and J. W. Kirchner (2000), Stress partitioning in streams by large woody debris, *Water Resour. Res.*, *36*, 2373–2379.

Mao, L., G. P. Uyttendaele, A. Iroume, and M. A. Lenzi (2008), Field based analysis of sediment entrainment in two high gradient streams located in Alpine and Andine environments, *Geomorphology*, *93*, 368–383.

Meyer-Peter, E., and R. Müller (1948), Formulas for bed-load transport, *Proceedings 2nd Congress*, pp. 39–64, Int. Assoc. of Hydraul. Res., Stockholm.

Millar, R. G. (1999), Grain and form resistance in gravel bed rivers, *J. Hydraul. Res.*, *37*, 303–312.

Mueller, E., J. Pitlick, J., and J. M. Nelson (2005), Variation in the reference Shields stress for bed load transport in gravel bed streams and rivers, *Water Resour. Res.*, *41*, W04006, doi:10.1029/2004WR003692.

Nikora, V., D. Goring, I. McEwan, and G. Griffiths (2001), Spatially averaged open-channel flow over rough bed, *J. Hydraul. Eng.*, *127*(2), 123–133.

Parker, C., N. J. Clifford, and C. R. Thorne (2011), Understanding the influence of slope on the threshold of coarse grain motion: Revisiting critical stream power, *Geomorphology*, *126*, 51–65.

Parker, G., P. C. Klingeman, and D. G. McLean (1982), Bedload and size distribution in paved gravel bed streams, *J. Hydraulic Div. ASCE*, *108*, 544–571.

Pitlick, J., E. R. Mueller, C. Segura, R. Cress, and M. Torizzo (2008), Relation between flow, surface-layer armoring and sediment transport in gravel bed rivers, *Earth Surf. Processes Landforms*, *33*, 1192–1209.

Raupach, M. R., D. A. Gillette, and J. F. Leys (1993), The effect of roughness elements on wind erosion threshold, *J. Geophys. Res.*, *98*(D2), 3023–3029.

Recking, A. (2009), Theoretical development on the effects of changing flow hydraulics on incipient bed motion, *Water Resour. Res.*, *45*, W04401, doi:10.1029/2008WR006826.

Rickenmann, D. (1991), Hyperconcentrated flow and sediment transport at steep slopes, *J. Hydraul. Eng.*, *117*(11), 1419–1439.

Rickenmann, D. (2001), Comparison of bed load transport in torrents and gravel bed streams, *Water Resour. Res.*, *37*, 3295–3305.

Rickenmann, D., and A. Recking (2011), Evaluation of flow resistance in gravel bed rivers through a large field data set, *Water Resour. Res.*, *47*, W07538, doi:10.1029/2010WR009793.

Ryan, S. E., L. S. Porth, and C. A. Troendle (2005), Coarse sediment transport in mountain streams in Colorado and Wyoming, USA, *Earth Surf. Processes Landforms*, *30*, 269–288.

Shields, A. (1936), Application of similarity principles and turbulence research to bed-load movement (in German), *Mitteil. Preuss. Versuchanst. Wasser, Erd, Schiffsbau*, vol. 26, Preußischen Versuchsanstalt für Wasserbau, Berlin.

Shvidchenko, A. B., and G. Pender (2000), Initial motion of streambeds composed of coarse uniform sediments, *Proc. Inst. Civ. Eng.*, *142*, 217–227.

Shvidchenko, A. B., G. Pender, and T. B. Hoey (2001), Critical shear stress for incipient motion of sand/gravel streambeds, *Water Resour. Res.*, *37*, 2273–2283.

Wathen, S. J., R. I. Ferguson, T. B. Hoey, and A. Werritty (1995), Unequal mobility of gravel and sand in weakly bimodal river sediments, *Water Resour. Res.*, *31*, 2087–2096.

Wiberg, P. L., and J. D. Smith (1991), Velocity distribution and bed roughness in high-gradient streams, *Water Resour. Res.*, *27*, 825–838.

Wilcox, A. C., J. M. Nelson, and E. E. Wohl (2006), Flow resistance dynamics in step-pool channels: 2. Partitioning between grain, spill, and woody debris resistance, *Water Resour. Res.*, *42*, W05419, doi:10.1029/2005WR004278.

Yager, E. M., J. W. Kirchner, and W. E. Dietrich (2007), Calculating bed load transport in steep boulder bed channels, *Water Resour. Res.*, *43*, W07418, doi:10.1029/2006WR005432.

Zimmermann, A. (2010), Flow resistance in steep streams: An experimental study, *Water Resour. Res.*, *46*, W09536, doi:10.1029/2009WR007913.

R. I. Ferguson, Department of Geography, Durham University, Durham DH1 3LE, UK. (r.i.ferguson@durham.ac.uk)